



Numerical analysis of tooling design for extruding wide aluminium hollow profiles using multi-container extrusion technology

Jiaxin Lv¹ · Zhusheng Shi¹ · Junquan Yu² · Weishu Li¹ · Jianguo Lin¹

Received: 4 July 2023 / Accepted: 12 September 2023 / Published online: 2 October 2023
© The Author(s) 2023

Abstract

Recently a novel multi-container extrusion method has been proposed and proved feasible to simultaneously extrude multiple billets for producing thin-walled wide profiles with reduced force by experiments. Due to its different die structure compared to conventional extrusion methods, the effects of tooling geometries on the multi-container extrusion performance should be comprehensively analysed as the base of die design optimisation. In this study, the original three-container extrusion design and six modified designs were established to investigate the influence of three key geometrical variables, including container diameter, upper die height and welding chamber height, on the extrusion performance through finite element simulation. The considered extrusion performances include metal flow uniformity, extrusion force, welding pressure, die lifetime and material yield. The drawbacks of the original die design were revealed after the primary analysis of the key influencing variables and a three-step way of design improvement was proposed accordingly. Container block and upper die were optimised for the first step; welding chamber height and die bearing length were modified during the second and third steps respectively. Compared with the original design, the final optimised design can decrease the unevenness of the extrudate front shape by 75% and double the material yield, while the extrusion force, die lifetime and welding quality were basically unchanged.

Keywords Three-container extrusion · Aluminium alloy · Material flow · Tooling optimisation · Numerical simulation

Introduction

Aluminium alloys have been widely used in the domains of aircraft [1], automobile [2] and marine [3] thanks to their superior properties including high specific strength, high corrosion resistance, good electrical and thermal conductivity, and so on. Extrusion is one of the major metal-forming technologies especially for producing complex cross-sectional shape such as the hollow wallboard of high-speed train [4] and ship deck [3]. Since the assembly and joining processes of small parts can be minimised by directly

manufacturing integral components, large-sized aluminium products are increasingly in demand to maintain better product quality and less energy consumption. The technical development of large-scale aluminium extrusions with complex cross-sectional shape hence becomes critical.

Porthole extrusion is a conventional method for manufacturing hollow profiles. Metal flow balance, welding defects, extrusion force, and tooling strength, are the key factors that need to be taken seriously in the porthole extrusion process [5, 6]. The uniformity of metal flow can be represented by σ_{stan} or velocity relative difference (VRD) as shown in Eqs. (1) and (2) [7, 8].

$$\text{SDV} = \sqrt{\sum_{i=1}^n \frac{(v_i - \bar{v})^2}{n}} \quad (1)$$

$$\text{VRD} = \frac{\sum_{i=1}^n \frac{|v_i - \bar{v}|}{\bar{v}}}{n} \quad (2)$$

where v_i is the velocity at node i , \bar{v} is the average velocity of all nodes, and n is the number of nodes in total. Lower

✉ Zhusheng Shi
zhusheng.shi@imperial.ac.uk

✉ Junquan Yu
junquan.yu@sdu.edu.cn

¹ Department of Mechanical Engineering, Imperial College London, London SW7 2AZ, UK

² Key Laboratory for Liquid-Solid Structural Evolution and Processing of Materials (Ministry of Education), Shandong University, Jinan, Shandong 250061, People's Republic of China

SDV or VRD represents a more balanced metal flow which results in a better quality of extrudate. Otherwise, poor uniformity can cause various product defects such as twisting, waving, bending and cracking [4]. Welds are intrinsic defects for hollow extrusions and are often the weakest part of the extruded profile. Welding property is usually evaluated by the contacting pressure on welding plane p or the ratio of pressure to effective stress $p/\bar{\sigma}$, where higher p or $p/\bar{\sigma}$ indicates better welding quality [9]. Good metal flow uniformity and welding property are crucial for qualified extrusion products. In the meantime, the extrusion force and the peak stress applied on extrusion dies are also critical indices which influence the availability of extruder and the extrusion die lifetime, respectively [10]. All these indices of extrusion performance can be influenced by modifying the extrusion tooling designs as listed in Table 1. With the aid of numerical simulations, the effects of different die design variables on extrusion performances are analysed more and more comprehensively [12].

For the container design in porthole extrusion, a larger container diameter and longer length allow more billet to be extruded at once, resulting in higher deformation-induced force and friction force [23]. The determination of container diameter is highly restricted by the desired extrudate and the container length is empirically set as 2–5 times the container diameter [11]. Therefore, more research is focused on the designs of upper die and lower die which contain a large number of critical geometrical variables. The key aspects of the upper die include the design of the porthole and bridge. Chen et al. [12] obtained the improved metal flow uniformity and welding property by numerical simulations of various modified die designs to extrude a multi-cavity wallboard profile for high-speed trains. The results demonstrated that

the shapes and locations of portholes should match the counterpart areas of the extrudate to ensure smooth metal flow. By smoothing the metal flow, extrusion force and peak stress on tools would also be reduced [20]. Donati et al. [13] compared the extrusion performances for different designs of bridge shapes experimentally and numerically and found that the bridge back angle of 45° can lead to better welding quality than a square bridge (bridge back angle equals 90°). The sharper bridge increases the welding pressure and welding path length simultaneously and hence yields good welding [14–16]. The bridge-mandrel connection is usually the riskiest area that encounters the highest stress, so the bridge-mandrel connecting fillet radius is also a tiny but important variable during extrusion [5]. The key parameters of the lower die include the design of baffle, welding chamber and bearing. Baffle plates are not necessary parts of the lower die but are often added on the bottom of the welding chamber near the orifice to balance the metal flow by rationally increasing the flow resistance in the local area [17]. Increasing the welding chamber height can effectively improve welding quality by increasing the welding pressure and area of the welding plane [18]. But Liu et al. [14] pointed out that an extra-high welding chamber may increase the extrusion force and resist the metal flow toward the die orifice. Therefore, the determination of welding chamber height becomes of great importance. Adding a second-step welding chamber with a well-designed shape is another way to obtain even metal exit velocity. Sun et al. [19] analysed the extrusion processes with different second-step welding chamber shapes and heights and finally selected the optimal design for uniform metal exit velocity and high die lifetime. In addition, adjusting the bearing length distribution could sensitively influence the

Table 1 Key variables of tooling design and extrusion performance

	Tooling design		Extrusion performance
Container	<ul style="list-style-type: none"> • Diameter [11]; • Length [11]. 		Metal flow <ul style="list-style-type: none"> • SDV • VRD
Upper die	<ul style="list-style-type: none"> • Porthole: shape, location, dimension [12]; • Bridge: angle [13-16], dimension [12]; 	➔	Welding quality <ul style="list-style-type: none"> • Contacting pressure; • Ratio of pressure to effective stress;
Lower die	<ul style="list-style-type: none"> • Baffle: shape, location, dimension, height [17]; • Welding chamber: height [18], 2-step chamber [19]; • Bearing length [20-22]. 		Energy consumption <ul style="list-style-type: none"> • Extrusion force Die lifetime <ul style="list-style-type: none"> • Peak stress

metal flow [20]. By lengthening the bearing in smooth flow area and shortening the bearing in obstructed flow area, the final metal exit velocity could be effectively balanced [21]. Increasing bearing length may slightly increase the extrusion force by introducing more friction between material and die bearing, and increase the welding pressure by increasing the resistance of metal flow [22].

To solve the challenge of extremely high force requirement during large-scale profile extrusion, a novel extrusion method, namely multi-container extrusion technology has been proposed [24]. The key feature of this method is that multiple containers are arranged in a container block to insert multiple billets at the same time. In this case, the billets with a diameter much smaller than the width of the extrudate can be extruded simultaneously into a desired profile, leading to a much smaller extrusion ratio and hence a significantly reduced extrusion force. It should be noted that longitudinal welds are inevitably formed by bonding the adjacent billets inside the welding chamber of the die during the multi-container extrusion process. Therefore, welding quality evaluation of the multi-container extrusion is of great importance. So far, a series of three-container extrusion tests have been conducted and the recorded extrusion force was only about 15% of that for the conventional porthole extrusion to extrude the same profile [24], showing the great potential of the novel extrusion multi-container extrusion technology to form large-scale profiles. Additionally, microstructural and mechanical testing has been carried out on the three-container extruded profiles, and numerical simulations have been conducted to analyse the formation mechanism of welds. It has been demonstrated that good welding can be achieved beyond a certain distance away from the front end of the extrudates [25].

The special tooling structure of multi-container extrusion, i.e. multiple containers in one container block, causes the extrusion performance to be very different from conventional extrusion process. However, no research has been presented to investigate the effects of tooling designs on the multi-container extrusion performance. Proposing reliable guidance for tooling design optimisation plays a vitally important role in the industrial application of the novel multi-container extrusion method.

The main objective of this study is to investigate the influence of three key tooling geometries on the performances during the three-container extrusion process and propose guidance for tooling design improvement by numerical simulation. The virtual extrusion processes with the original and six modified tooling designs were performed by the software QForm. The three modified variables include container diameter, upper die height and welding chamber and the five extrusion performance indices to be analysed include metal flow, welding property, extrusion force, die lifetime and material yield. According to the results, the limitations

of the original extrusion design were investigated and three steps of tooling design improvement were subsequently conducted for better extrusion performance.

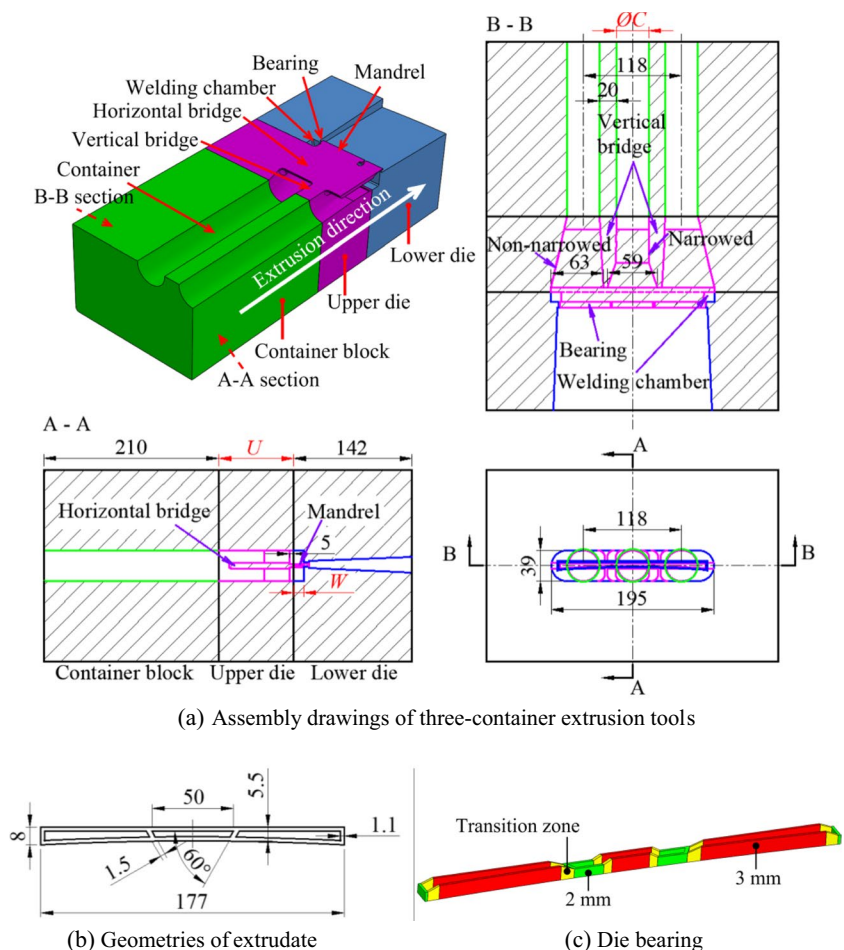
Numerical modelling of three-container extrusion process

Constructions of geometrical models

The three-container extrusion tooling set including container block (in green), upper die (in red) and lower die (in blue) is illustrated in Fig. 1a. The top left image shows 1/4 part of the 3-D model and the others show the 2-D drawings with detailed dimensions. Three cylindrical containers with a diameter of ϕC are arranged in a row at an equal spacing of 20 mm, and the centre distance between the left and the right container is 118 mm as shown in B-B section. The upper die includes three lofted portholes of which the total height is represented as U in A-A section. The entrances of the portholes are three the same circles as the container and the exits are rounded rectangular with the same width of 39 mm and with lengths of 63 mm or 59 mm shown as the red lines in bottom right drawing and top right B-B section. To ensure the safety of vertical bridges, i.e. the gaps between the portholes, the middle porthole was narrowed at the entrance so as to widen the vertical bridge as shown in the B-B section drawing. Additionally, a horizontal bridge is placed through the three portholes and connected with the mandrel to form the hollow area of extrudate during extrusion as shown in A-A section. The lower die includes a rounded welding chamber with a sectional area of 195 mm \times 39 mm and a height of W shown as the blue lines in the lower two figures of Fig. 1a. This die set is used to extrude a 177 \times 8 mm \times 1.1 mm hollow profile with two 1.5 mm thick reinforcing ribs as shown in Fig. 1b. The ribs spaced 50 mm apart connect the flat top surface and curved bottom surface with an inclination of 60°. The distance between the top and bottom surface ranges from 5.5 mm to 8 mm. Figure 1c shows the bearing length distribution on the die orifice where most is 3 mm (in red) while those near the reinforcing ribs and short edges are shorter (2 mm, in green). The connecting parts between the 3 mm and 2 mm bearings are transited by chamfers.

An original die in the authors' previous work [24, 25] was designed based on engineering expertise of traditional porthole die design, and the corresponding extrusion experiments were successfully conducted to produce wide-thin aluminium profiles. The subsequent simulation indicated that while the design was capable of ensuring a successful extrusion process, but fell short for achieving an optimal outcome, requiring further analysis of the effect of die structures. As shown in Fig. 1, the main die structural parameters include container diameter, and the cross-sectional

Fig. 1 Three-container extrusion die design



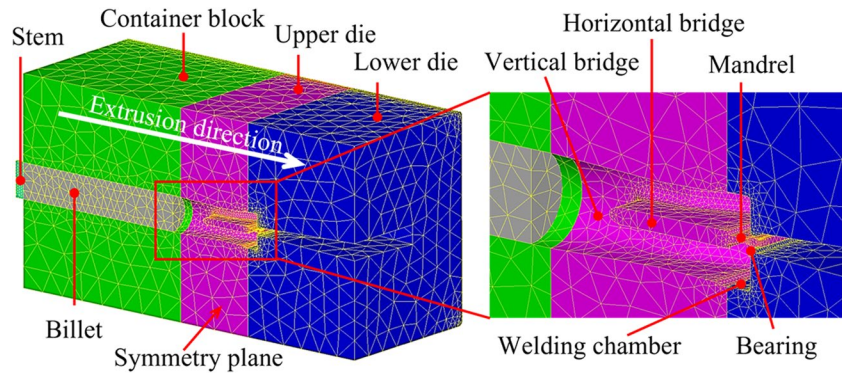
shapes and heights of both the upper die and the welding chamber. The optimal determination of the cross-sectional shapes of the upper die and the welding chamber can be largely guided by the existing design handbook based on the principle that the secondary extrusion ratio at different positions of the cross-section should be the same [11]. Therefore, three other variables, i.e. container diameter ϕC , upper die height U and welding chamber height W in Fig. 1 are selected as the key parameters to analyse their effects on three-container extrusion performance. Table 2 lists the detailed values of the selected parameters for the original die design and six modified designs of which the modified parameter is marked in *italic bold*. Designs C1/C1' and C2/

C2' change the container diameter ϕC from the original 39 mm to 34 mm and 44 mm respectively. Designs U1 and U2 change the upper die height from the original 90 mm to 65 mm and 115 mm, respectively. Designs W1 and W2 modify the welding chamber height from the original 12 mm to 6 mm and 18 mm, respectively. It should be noted that Design C1 and C1' actually have the same tooling structure, so do Design C2 and C2'. The only difference is that Designs C1 and C2 have the same stem speed as that for the original design during the extrusion process, while Design C1' and C2' have the same extrudate exit speed as that for the original design. This will be explained in detail in "[Meshing & Boundary conditions](#)" section.

Table 2 Geometrical variables for the original design and Design C1 ~ W2

	Original design	Design C1/C1'	Design C2/C2'	Design U1	Design U2	Design W1	Design W2
ϕC (mm)	39	34	44	39	39	39	39
U (mm)	90	90	90	65	115	90	90
W (mm)	12	12	12	12	12	6	18

Fig. 2 FE model of the three-container extrusion process



Meshing & Boundary conditions

Different finite element (FE) models are established according to the die designs described in "Constructions of geometrical models" section. Taking the original design as an example, half of the extrusion system is built with a symmetry plane to reduce the computational load as shown in the left image of Fig. 2. The whole model includes stems, billets and die set which are meshed into tetrahedron elements. The way applied to constrain the element size in this study is mesh adaption with an acceleration coefficient. The mesh adaption is the ratio of the maximum element size to the size of any element in the finite mesh element, of which the maximum and maximum values are set as 1 and 15, respectively; the acceleration coefficient represents the maximum ratio of element sizes between neighbour elements, which is set as 1.5 in this study. The detailed element sizes for each simulation step are determined by the solver based on the real-time dimensions and shape of the tooling and workpiece. Although the original mesh size of the billets may look coarse, it will be automatically decreased by remeshing. The maximum strain increment for each simulation step is 0.1 and the maximum step time is 0.5 s. The maximum number of steps between remeshing is 20. During the simulation,

the die set is fixed and the stems push the billets to move forward along the extrusion direction.

As reported in the previous study [24], the initial temperatures of extrusion tools and billets were set the same during the extrusion experiments for uniform temperature distribution. The extrusion temperature in the numerical models is in accordance with the extrusion experiment, i.e. 450 °C. The stem speed during the simulation of Design C1, C2, U1, U2, W1 and W2 were the same as the original extrusion, i.e. 0.5 mm/s. Since changing the container diameter while keeping the original stem speed for Designs C1 and C2 leads to the change of the extrudate exit velocity and strain rates in the weld chamber, extra two simulations of C1' and C2' were conducted to compare the influence of the container diameter at the same extrudate velocity. The extrusion conditions of all the simulations are summarised in Table 3.

The billet and tooling materials are AA6063 alloy and H13 tool steel, respectively, whose physical properties are listed in Table 4. The flow stress σ_s for AA6063 material is formulated as,

$$\sigma_s = A \cdot e^{m_1 T} \cdot \epsilon^{m_2} \cdot \epsilon^{m_4/\epsilon} \cdot (1 + \epsilon)^{m_5 T} \cdot \epsilon^{m_3} \tag{3}$$

Table 3 Extrusion conditions of different simulations

Design	Original	C1	C2	U1	U2	W1	W2	C1'	C2'
Stem speed (mm/s)	0.5	0.5	0.5	0.5	0.5	0.5	0.5	0.66	0.39
Extrusion temperature (°C)	450								

Table 4 Physical properties of materials of billet and extrusion tools

Material	Young's modulus (MPa)	Poisson's ratio	Density (kg/m3)	Thermal conductivity [W/(m·K)]	Specific heat [J/(kg·K)]
AA6063	70600 – 51.25T	0.33 + 6.25 × 10 ⁻⁵ T	2699 – 0.235T	205 + 0.0875T	904 + 0.2542T
H13 tool steel	210000	0.3	7716	29	551

where ϵ and $\dot{\epsilon}$ are strain and strain rate respectively; T is the temperature; $A, m_1, m_2, m_3, m_4, m_5$ are all material constants, equal to 265 MPa, -0.00458, -0.12712, 0.12, -0.0161, and 0.00026, respectively [26]. The yield stress of H13 tool steel decreases with temperature and is 1150 MPa at 450 °C according to the QForm material database [26].

The heat transfer coefficient between the workpiece (billet) and tools is 30000 W/(m²·K); the heat transfer coefficient between the workpiece/tool and the environment is 30 W/(m²·K) [27]. The friction τ between the workpiece and the inner wall of the die obeys Levanov’s law, i.e.

$$\tau = mk \left[1 - \exp\left(-b \frac{\sigma_n}{\sigma_s}\right) \right] \tag{4}$$

where k is the maximum shear stress equal to $\frac{\sigma_s}{\sqrt{3}}$; σ_n is the contact pressure; m is the friction factor; b is the

experimental coefficient. m and b were respectively set as 1 and 1.25 in this study.

Validation of numerical simulation

To confirm the correctness of the FE model, Fig. 3 compares the simulated extrusion force for the original die design with the corresponding experimental results from the previous work [24] and similar evolving trends were obtained. The extrusion force initially increases to satisfy the energy requirement of billet upset and entering the upper die; then the force decreases slightly when passing through the upper die and rises again when filling the welding chamber; after filling the dies, the materials start to break through the die bearing with a dramatically increase of extrusion force; finally, the materials are extruded out of the orifice to form the desired profile. Except for the similar force evolving trend, the predicated maximum extrusion, 2438 kN, is also close to the experimental result, 2224 kN. Therefore, it can be concluded that the established FE model is validated and the simulated results are reliable.

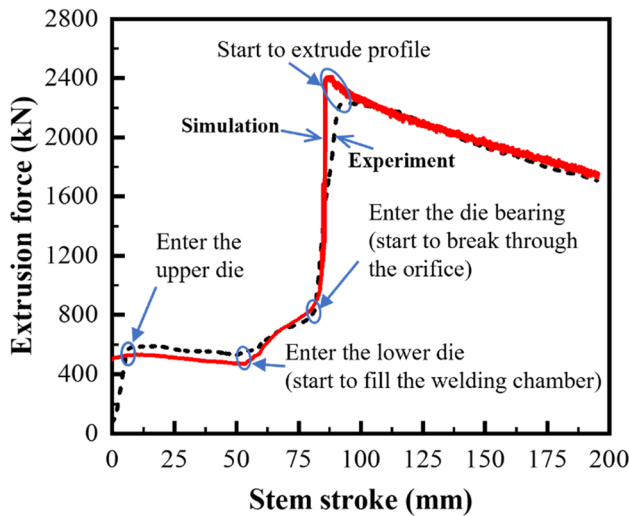


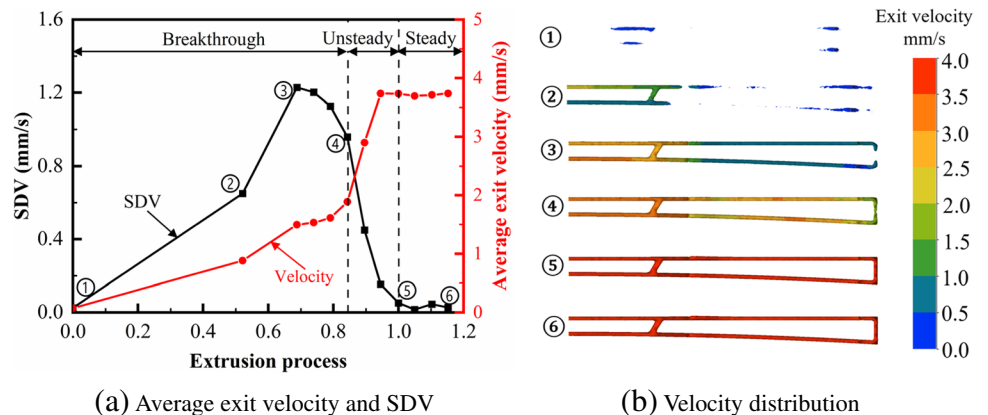
Fig. 3 Comparison of extrusion forces obtained from numerical simulation (solid line) and experiment (dashed line)

Effects of tool designs on extrusion performances

Preliminary analysis

The metal flow behaviour through the die orifice for the extrusion with the original tooling design is presented in Fig. 4, where Fig. 4a shows the evolution of the average exit velocity and SDV during the extrusion process and Fig. 4b shows the exit velocity distribution in the cross-section of the orifice at different times of extrusion. The “extrusion process” axis in Fig. 4a is a non-dimensional time normalised by the starting time of the steady extrusion, which presents the extrusion progress from the beginning of material passing through the die orifice (=0) to the beginning of flowing with steady velocity (=1) and further (>1). The

Fig. 4 Metal flow process including breakthrough stage (①–④), unsteady stage (④–⑤) and steady stage (⑤–⑥) during the extrusion process of the original design



images ①–⑥ in Fig. 4b correspond to the six points of extrusion in Fig. 4a. At point ①, the material starts to flow through the orifice very slowly and only a few dispersed materials can be observed on the cross-section. At point ②, more material is extruded with increasing exit velocity and SDV. At point ③, the top and bottom surfaces of the extrudate have been extruded, where the middle part flows much quicker than the side part and the SDV increases to the maximum value. At point ④, material eventually breaks through the whole orifice and an entire cross-section is extruded with a gradually improved flow uniformity. The process ①–④ covers the whole material breakthrough stage during which the average exit velocity gradually increases and SDV increases first and then decreases. After that is the unsteady stage, during which the entire profile is extruded non-uniformly with a decreasing SDV and increasing average exit velocity until point ⑤. During the steady stage after point ⑤, the material can be extruded steadily and uniformly.

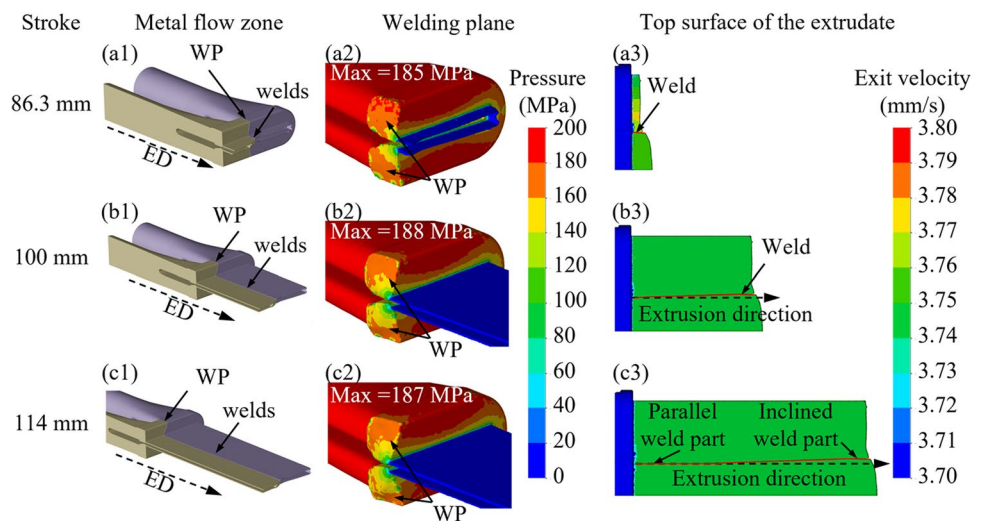
The simulated metal flow during the steady stage extrusion of the original design is illustrated in Fig. 5, where the images (a1 – a3) present the situation at the beginning of steady extrusion, i.e. when the stem stroke is 86.3 mm and the non-dimensional extrusion process equals 1; the images (b1 – b3) and the images (c1 – c3) correspond to the extrusion at the stem stroke of 100 mm and 114 mm, respectively. As shown in the image (a1), the materials from two billets as indicated in taupe (front) and purple (back) respectively are contacted and bonded together after fully filling the die cavity, resulting in the formation of the welding plane. The bonded material is then extruded through the die orifice to form the final extrudate, accompanied by two longitudinal welds at the top and bottom surfaces of the extrudate. These welds formed by the solid-state bonding between the adjacent billets are intrinsic and unique defects during the multi-container extrusion process compared to other extrusion methods. Therefore, the physical state of the welding plane

is of great importance to evaluate the welding quality of the final multi-container extruded profile. The images (a2), (b2) and (c2) show the pressure distributions of the side billet, corresponding to the purple billet in images (a1), (b1) and (c1), and the maximum pressures on the welding plane are marked. The welding pressure distributions in images (a2), (b2) and (c2) appear approximately unchanged so one can assume that the physical state of the welding plane during steady extrusion is consistent. The exit velocity distributions at different extrusion strokes are shown in images (a3), (b3) and (c3). Except that the image (a3) shows a slight velocity gradient within the range of 3.7–3.8 mm/s with the SDV value of 0.05 at the beginning of steady extrusion, the exit velocity distributions are nearly perfectly uniform during the further steady stage extrusion.

To sum up, the non-uniformity of the metal flow is mainly influenced by the extrusion process before the steady stage, so the breakthrough and unsteady stages were focused on for the investigation of the metal flow. Evaluating the bonding quality of the weld formed between the adjacent billets is important for the multi-container extrusion and almost all the usable profile is extruded during the steady extrusion process, so the steady stage was focused on when analysing the welding plane. In addition, according to "Validation of numerical simulation" section, the extrusion force reaches the maximum value at the end of the breakthrough stage when the die is in the severest safety danger, so the end of the breakthrough stage should be focused on for the evaluation of the die lifetime.

Moreover, the shape of the welding plane evolves with the stem stroke, and the corresponding weld position is not exactly parallel with the extrusion direction as shown in the image (b2) and (b3). This is caused by the unbalanced material distribution in the welding chamber due to the volume difference between the two flow portholes for the side billet and the middle billet as depicted in Fig. 1a. The middle

Fig. 5 Steady stage of the three-container extrusion process for the original design, showing (a1–c1) the formation of welds, (a2–c2) stable physical state of welding plane and (a3–c3) evolution of weld position. ED and WP stand for extrusion direction and welding plane respectively



porthole was narrowed to enhance the safety of the vertical bridges, but it also caused a decreased middle porthole volume compared to the side porthole. Therefore, as shown in Fig. 5, the material from the middle (taupe) billet arrives in the welding chamber prior to the side (purple) billet and hence occupies a larger portion of the cross-section of the extrudate. With the increasing stem stroke, sufficient material from the side billet arrives in the welding chamber, gradually taking back some flow area of the welding chamber and part of the extrudate cross-section. Therefore, the weld position on the cross-section of extrudate gradually moves inward from the side, leading to an inclined weld seam relative to the extrusion direction on the surface of the extrudate as shown in the image (b3). The evolving material distribution finally gets stable and the weld seam on the subsequent extruded profile turns to be parallel with the extrusion direction as shown in the image (c3).

Metal flow behaviour and extrusion force

The simulated evolutions of average exit velocity and SDV for the modified extrusion designs described in "Constructions of geometrical models" section are plotted in Fig. 6. Same as in Fig. 4, the non-dimensional "extrusion process" axis reflects the extrusion progress after the billet material fully fills the whole die cavity, i.e. from the beginning when the material starts to be extruded through the die orifice. All designs obey the same evolving trend of average exit velocity, i.e. increasing during the breakthrough and unsteady stage and finally reach the plateau as shown in Fig. 6a. Modifying the upper die height (Designs U1 and U2) and welding chamber height (Designs W1 and W2) has little influence on the steady velocity; decreasing or increasing the container diameter in Design C1 or Design C2 can significantly reduce or increase the steady exit velocity due to the change of extrusion ratio, and by adjusting the stem speed, the steady exit velocity can be changed to the original level as shown in curves C1' and C2'. In Fig. 6b, all curves show a similar evolving trend, i.e. the SDV increases up

to the peak and then decreases quickly to low values at the steady state extrusion.

Although the value of SDV in the steady stage (extrusion process ≥ 1) is almost the same for different designs as demonstrated in Fig. 6b, the previous values are not identical, resulting in the different front-end shapes of the extruded profiles as shown in Fig. 7. The unevenness of the front shape is quantified by the length of the extrudate front edge along extrusion direction, l , and the material distribution in the extrudate is quantified by the width of the extrudate portion formed by the middle billet. For all the designs, the middle part of extrudate front shape is bulgy because the volume of the middle porthole of the upper die is smaller than that of

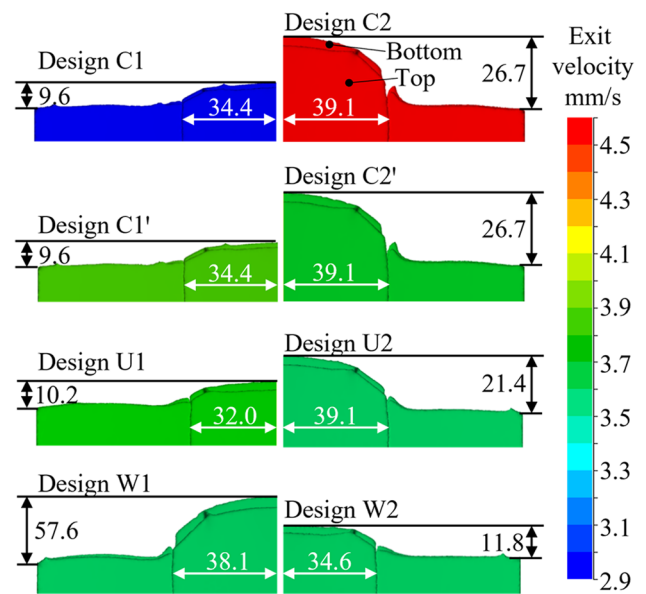
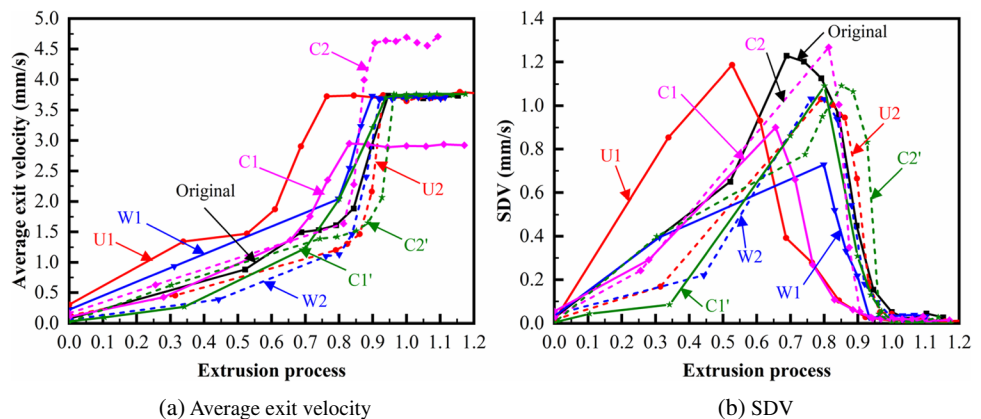


Fig. 7 Front shapes of profiles extruded by different tool designs, where the colours show the exit velocity distribution; the numbers in black (in mm) indicate the length of the extrudate front edge along extrusion direction l ; the numbers in white (in mm) represent the width of the extrudate portion formed by the middle billet; the labels of 'Top' and 'Bottom' represent the top surface and bottom surface of the extrudate which are marked for Design C2 as an example

Fig. 6 Average exit velocity and SDV from breakthrough stage to steady stage for different extrusion designs. Extrusion process equal to 1 represents the beginning of the steady extrusion



the side porthole as annotated in Fig. 1a. From Fig. 7, it can be seen that with the same die structures, both the increase (from Design C1 to C1') and the decrease (from Design C2 to C2') in extrusion speed exert minimal influence on the unevenness of the front shape. With larger container diameter (Design C2/ C2'), higher upper die height (Design U2) or lower welding chamber height (W1), the volume difference between the middle and side portholes becomes larger and hence the middle material can reach the die orifice quicker and earlier, resulting in a more uneven front shape and wider portion of extrudate formed from the middle billet. This gives the first idea of tooling design improvement: making the metal flow volumes of multiple portholes equal so as to ensure the materials from different billets can begin to be extruded at the same time. In addition, the top surface of the extrudate is more salient than the bottom surface, which means that after the material is divided into top and bottom parts by the horizontal bridge, the top material reaches the

die orifice earlier than the bottom material. Accordingly, the second idea of tooling design improvement can be made: adjusting the location of the horizontal bridge to ensure an equal metal flow volume for top and bottom materials.

Figure 8 shows the simulated maximum extrusion forces for different designs, corresponding to the point ④ of Fig. 4, and the normalised values by the maximum extrusion force of the original design (2438 kN). Decreasing upper die height (Design U1) and welding chamber height (W1) can reduce the extrusion force slightly mainly due to the reduction of friction between the material and die interface. Decreasing container diameter (Design C1/C1') can markedly decrease the extrusion force. Smaller container diameter indicates a lower extrusion ratio and hence leads to lower deformation induced force. For the same reason, C2/C2' with larger diameter have larger extrusion forces.

Welding pressure

The contacting pressure distributions on the welding plane formed by the bonding of the adjacent billets for different extrusion die designs are shown in Fig. 9. The pressure is minimum at the outlet and gradually increases along the direction away from it. Compared to Design C1/C2', higher stem speed in Design C1'/C2 can slightly increase the welding pressure. Smaller container diameter (Design C1/C1') leads to lower pressure compared to Design C2/C2' which is coincident with its influence on extrusion force. Similarly, lower upper die height (Design U1) leads to slightly lower pressure compared to Design U2. Decreasing welding chamber height (Design W1) slightly increases the welding pressure compared with Design W2. However, according to the related literature, decreasing welding chamber height

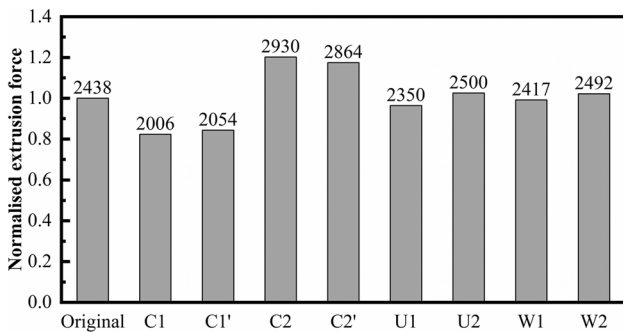
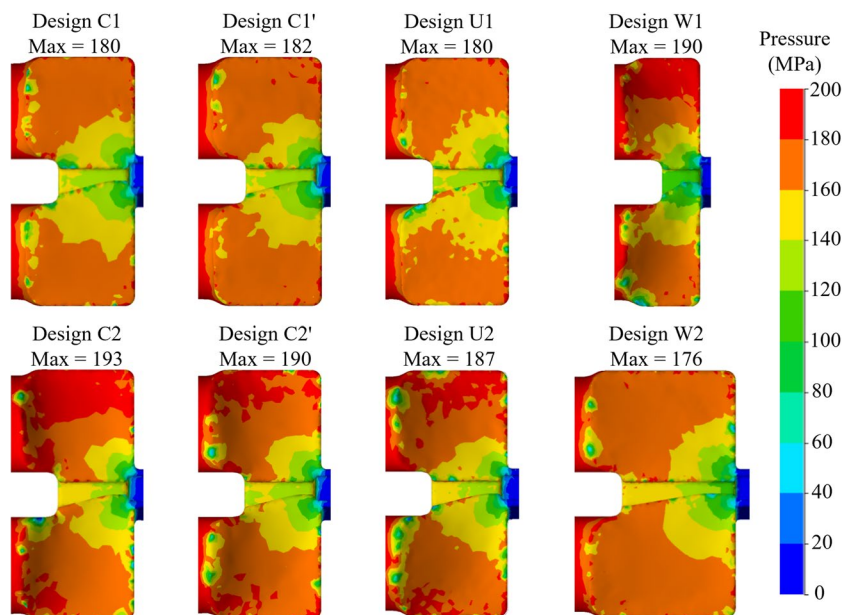


Fig. 8 Normalised extrusion force at steady state extrusion process for different die designs, where the number (in kN) on the top of each bar represents the corresponding values of extrusion force

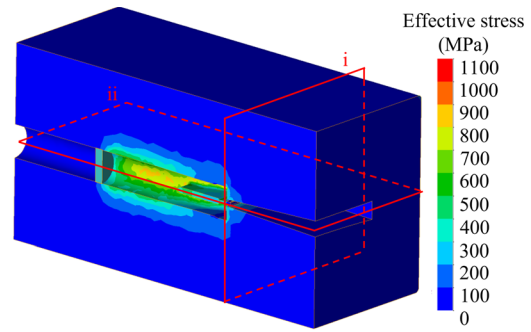
Fig. 9 Pressure distribution on the welding plane for different extrusion designs



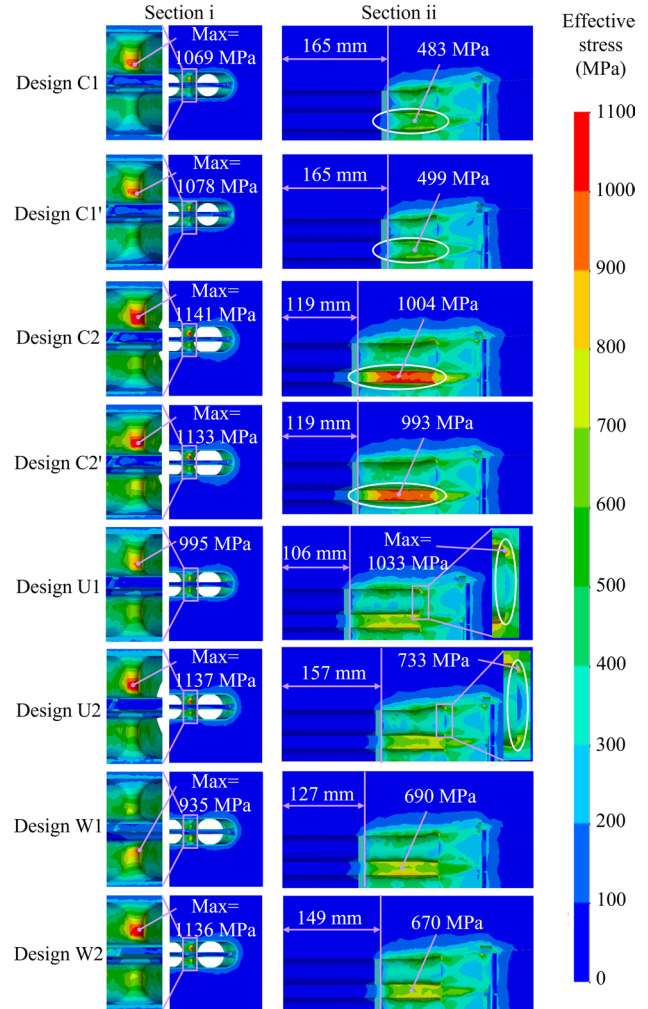
makes the welding paths and welding times reduced which worsens the welding quality [28]. In addition, it has been demonstrated that the ratio of welding pressure to effective stress serves as a superior index for assessing welding quality compared to the welding pressure alone. The detailed interplay between welding pressure and effective stress will be examined in "Design 3: improvement of bearing lengths" section as part of the tooling optimisation process. It should also be noted that as long as the welding condition satisfies the limit of forming sound welds, higher welding pressure or longer welding path and time become unnecessary.

Die lifetime and material yield

Figure 10 illustrates the effective stress distributions of the whole die set, including a container block, an upper die and a lower die, for different extrusion designs when the extrusion force reaches the maximum, i.e. at the end of the breakthrough stage. Figure 10a depicts the detailed positions of the analysed cross-sections by using the original extrusion tooling as an example, of which Section i is perpendicular to the extrusion direction and Section ii is the horizontal plane over the centre line of the containers. Figure 10b shows the effective stress distribution on the indicated cross-sections for the different modified die designs where the corresponding peak stress and stem strokes are also marked. In the case of applying the same stem speed, the die with a bigger container diameter (Design C2) encounters much higher stress than Design C1, where the peak stress increases from 1069 to 1141 MPa, and the stress on the gap of containers significantly increases from 483 to 1004 MPa. Similar effects of container diameter can be obtained in the case of applying the same extrudate exit velocity according to the comparison between Design C1' and C2'. Besides, the bigger container diameter in Design C2/C2' allows more volume of billet to be extruded and hence shortens the necessary stem stroke of filling the die cavity from 165 mm for Design C1/C1' to 119 mm for Design C2/C2'. Compared to Design U1, the longer upper die height in Design U2 increases the stress on the vertical bridge end from 995 to 1137 MPa, while decreasing the stress on the horizontal bridge as shown in the circled area from 1033 to 733 MPa. The advantage of Design U1 is that the smaller volume of the die cavity reduces the requirement of stem stroke for filling the whole die cavity, resulting in higher material yield. It should also be noted that the riskiest part in Design U1 changes from the end of the vertical bridge to the entrance of the horizontal bridge. Compared to Design W1, the larger welding chamber height in Design W2 causes higher localised stress on the vertical bridge end from 935 to 1136 MPa and slightly lower stress on the horizontal bridge from 690 to 670 MPa. Design W2 also maintains a larger volume of die cavity resulting in the reduction of material yield.



(a) Schematic of cross-section planes



(b) Effective stress on Sections i and ii

Fig. 10 Effective stress distribution for different extrusion designs, where the numbers in MPa and in mm represent the applied effective stress and stem stroke at the maximum extrusion force respectively

Table 5 summarises the normalised extrusion performance indices of different tooling designs by that of the original design according to the above-mentioned analysis. The unevenness of the extrudate front shape is highly influenced by the die

Table 5 Performances of the original design and the six modified designs

Design	Original	C1	C1'	C2	C2'	U1	U2	W1	W2
Unevenness of the front shape, <i>l</i>	1	0.77	0.77	2.16	2.16	0.82	1.73	4.66	0.96
Maximum extrusion force	1	0.82	0.84	1.20	1.17	0.96	1.03	0.99	1.02
Maximum welding pressure	1	0.97	0.98	1.04	1.02	0.97	1.01	1.02	0.95
Peak stress on extrusion dies	1	0.98	0.98	1.04	1.03	0.94	1.04	0.85	1.04
Material yield	1	0.55	0.55	1.27	1.27	1.47	0.67	1.14	0.80

structure and the underlying reason is the unbalanced material distribution when materials flow into the welding chamber. The extrusion force can be greatly increased with larger container diameter mainly due to the higher extrusion ratio and affected by the increased strain rate, while the influence of the geometry of the upper die and welding chamber is little, i.e. within 4% in this case. The pressure on the welding plane between the adjacent billets is only slightly affected by all the structural modifications. But the welding path can be greatly influenced by the welding chamber so the evaluation of the welding quality should be researched particularly during the tooling optimisation. Unless the gap between the adjacent containers is too low, the peak stress of the extrusion dies mainly locates on the end of the vertical bridge due to the pressure in the welding chamber or on the entrance of the horizontal bridge induced by the material separation. Therefore, decreasing the upper die height or increasing the welding chamber height may increase the tooling risk. Increasing material yield can be achieved by either increasing the volume of the containers or decreasing the volume of the upper die and welding chamber.

By comparing the results in Table 5 and a tooling optimisation case for traditional porthole die in [29], it can be concluded that die features influence multi-container extrusion in a similar way to porthole extrusion. Increasing the container size results in elevated extrusion force and heightened stress on dies for both types of extrusion. Moreover, in the context of multi-container extrusion, a pronounced susceptibility exists in relation to larger container diameters, particularly in the gap zone between adjacent containers. Additionally, larger container diameters, higher upper die heights, and lower welding chamber heights can adversely affect the uniformity of metal flow in multi-container extrusion which is a phenomenon not as evident in porthole extrusion.

Tooling design improvement

According to the investigation of die design effects above, two main drawbacks of the original extrusion are identified: the uneven front shape of extrudate due to the non-uniform metal flow during both the breakthrough and unsteady extrusion stage and lower material yield. To improve these, the original die design is modified under

the premise of not raising the required extrusion force, keeping the peak stress of the die lower than its yield stress (1100 MPa) and maintaining good welding quality. Considering the impact sensitivity of different variables, the die design was improved by three steps where container block and upper die were first improved in Design 1, the welding chamber height was then modified in Design 2 and finally the bearing length was modified in Design 3. It should be noted that extrusion processes for the following improved designs are only simulated with the same stem speed, i.e. 0.5 mm/s.

Design 1: improvement of container block and upper die

Figure 11 shows the horizontal section (A-A) and vertical section (B-B) of the container block and upper die for Design 1 of which the section positions are illustrated in the 3D drawing (i). The drawing (ii) shows the die cavity of the container block in green and upper die in red. Compared with the original container shown with green dashed lines, a larger container diameter of 42 mm is applied in Design 1 as shown with the green solid lines. The upper die height is also shortened from the original 90 mm to 45 mm in Design 1. The narrowing of the lofted middle channel as shown in the blue dashed lines of drawing (ii) is eliminated to ensure the consistent metal flow volume for all three portholes. In addition, the diameters of the three containers are set equal in this study, leading to the equal volume flowrate of different portholes in the upper die. Repositioning both the horizontal and vertical bridges can balance the flow velocity inside the portholes. In this study, the horizontal bridge was moved down for 0.5 mm as shown in the drawing (ii) in Fig. 11 to make the volumes of metal flow for top and bottom materials equal. The key features of the original and the improved designs are listed in Table 6 in which the modified variables are marked in italic bold.

The extrusion process is simulated using the same boundary conditions and processing parameters as in the previous simulations. The simulated front shape of extrudate is shown in Fig. 12. The extrusion velocity of Design 1 increases from 3.8 mm/s for the original design to 4.3 mm/s because of

Fig. 11 Modified container block and upper die of Design 1

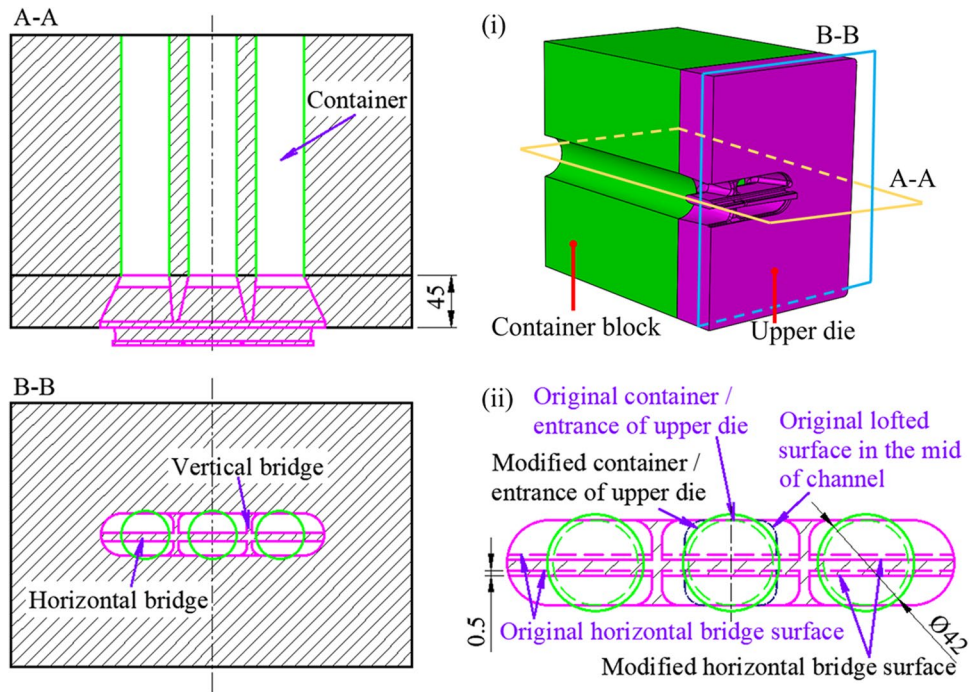


Table 6 Geometrical variables for the original design and improved Designs 1–3

	Original design	Design 1	Design 2	Design 3
Container diameter, ϕC (mm)	39	42	42	42
Upper die height, U (mm)	90	45	45	45
Flow area of upper die	Uneven volume in portholes	[Similar volume in portholes]	Similar volume in portholes	Similar volume in portholes
Welding chamber height, W (mm)	12	12	6	6
Bearing lengths, b (mm)	2–3	2–3	2–3	2~5

the increase in container diameter. The length of front edge along the extrusion direction l decreases from 12.4 mm for the original design to 3.4 mm for Design 1, indicating the improvement of the metal flow during the breakthrough and unsteady extrusion stages. In addition, the width of the extrudate portion from the middle billet for the original design is 34.7 mm and the corresponding value for the three modified extrusion designs are all equal to 30.4 mm, indicating that the material distribution in the welding chamber has been balanced by the adjustment of the upper die structure.

Design 2: improvement of welding chamber

Based on Design 1, the welding chamber height of the lower die is shortened to 6 mm to furtherly increase the material yield in Design 2. Since the welding chamber can not only provide space for materials welding but also balance the material flow [30], the smaller volume of the welding chamber in Design

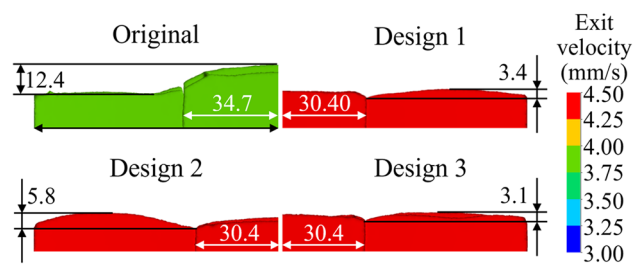


Fig. 12 Front shape of the extrudates for different extrusion designs. The colours indicate the exit velocity distribution; the numbers in black (in mm) indicate the length of the extrudate front edge along the extrusion direction l ; the numbers in white (in mm) represent the width of the extrudate portion formed by the middle billet

2 causes less flow uniformity. As shown in Fig. 12, the front shape of extrudate for Design 2 becomes more uneven than Design 1 which is consistent with the analysis result in Fig. 7.

Design 3: improvement of bearing lengths

Adjusting bearing lengths is typically employed as the final optimisation step for porthole extrusion. This is because changes in bearing lengths predominantly impact the uniformity of metal flow, while exerting a negligible influence on other extrusion performance indicators such as extrusion force and welding quality [11]. Therefore, although not examined in "Effects of tool designs on extrusion performances" section, the bearing length distribution is adjusted for Design 3 shown in Fig. 13 to further improve the metal flow uniformity. The bearing corresponding to the bulge area of the extrudate is lengthened from the original 3 mm to 5 mm as shown in red. The bearing length is 3 mm around the reinforcing ribs and 2 mm on both sides. With this non-uniform bearing length distribution, the most optimised front shape of extrudate can be obtained as shown in Design 3 of Fig. 12, with only a 3.1 mm long front edge.

In conclusion, the container diameter and the porthole shape of the upper die were modified in Design 1, which is the unique optimisation method for multi-container extrusion. The conventional optimisation method of changing the welding chamber was used in Design 2 to increase the material yield and the method of bearing length adjustment was applied in Design 3 to further balance the material exit velocity. This indicates that the application of the traditional tooling optimisation methods is also functional and efficient for the novel multi-container extrusion technique. At the same time, the proposed multi-container extrusion technique allows more flexibility in tooling design such as changing the structure of the container block. Although not considered in this study, changing the number and arrangement of containers can theoretically become another unique method for balancing the metal flow.

Comparison of the improved designs

The distributions of pressure and effective stress on the welding plane for Designs 1–3 are illustrated in Fig. 14. The ratio of welding pressure to effective stress is used to quantitatively evaluate the welding quality in this study, which can be formulated in discrete term [18] as,

$$Q = \frac{1}{n} \sum \frac{p_i}{\sigma_i} \quad (5)$$

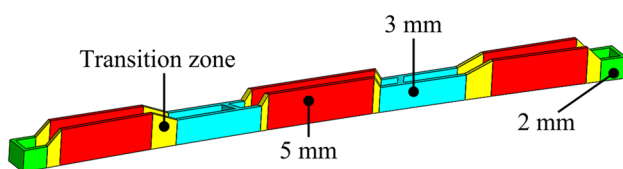


Fig. 13 Modified bearing lengths for Design 3

where p_i is the nodal welding pressure, σ_i is the nodal effective stress and n is the total number of nodes that are evenly distributed on the welding plane. The total number of nodes is 200 in this study. Table 7 summarises the ratio of average pressure to average effective stress $\frac{p_{ave}}{\sigma_{ave}}$ and Q -index for different extrusion designs. Compared with the original design, $\frac{p_{ave}}{\sigma_{ave}}$ and Q are decreased only less than 5% in Design 3. All values are higher than 6, i.e. the welding pressure is averaged over 6 times effective stress. It has been stated that if the ratio of pressure to effective stress exceeds approximately 3–4, good welding quality of aluminium profile can be ensured during extrusion [18]. Zhao et al. [31] conducted the extrusion test of aluminium alloy where the ratio of welding pressure to effective stress ranges from 0 to 4 and the extruded profile showed insufficient welding quality. On the contrary, good welding quality was obtained for another extruded product with an average ratio of welding pressure to effective stress higher than 5 [14]. Therefore, it can be concluded the Q -indices over 6 for all design schemes in the present study demonstrate that good welding can be formed.

Figure 15 shows the effective stress distribution of dies for the original design and improved designs when the extrusion force becomes the maximum, i.e. when the billets fill the whole die cavity. For the original design, the peak stress is 1095 MPa at the end of the top vertical bridge and the corresponding extrusion force is 2438 kN. It is obvious that stress on the top vertical bridge is higher than on the bottom vertical bridge, indicating the unsymmetric metal flow of the top and bottom materials. After the optimisation of the container block and upper die, the stress distributions of top and bottom vertical bridge become basically symmetric. The peak applied stress on Design 1 is 1092 MPa at the corner of the horizontal bridge and the maximum extrusion force is decreased to 2383 kN. By shortening the welding chamber height, Design 2 slightly reduces the peak stress to 1058 MPa and the maximum extrusion force to 2336 kN. With the modification of bearing length distribution, Design 3 leads to a slightly increased peak stress of 1073 MPa and maximum extrusion force of 2367 kN due to the increased friction when material passes through the bearing. The stem stroke needed to fully fill the whole die cavity is marked in Fig. 15 by which the material yield can be calculated. By increasing the container diameter and decreasing the upper die and welding chamber height, the stem stroke is changed from the original 136 mm to 78 mm for Design 1 and 68 mm for Design 2 and 3.

For better comparison, the above-mentioned extrusion performance indices of different designs are normalised by the values of the original design, so all the indices for the original design are 1 as shown in Table 8. Although the peak stress on the extrusion die and the maximum extrusion force is only decreased to a negligible extent, the unevenness of the front shape in Design 3 is greatly improved from

Fig. 14 Pressure and effective stress distribution on welding plane during steady extrusion for Designs 1–3

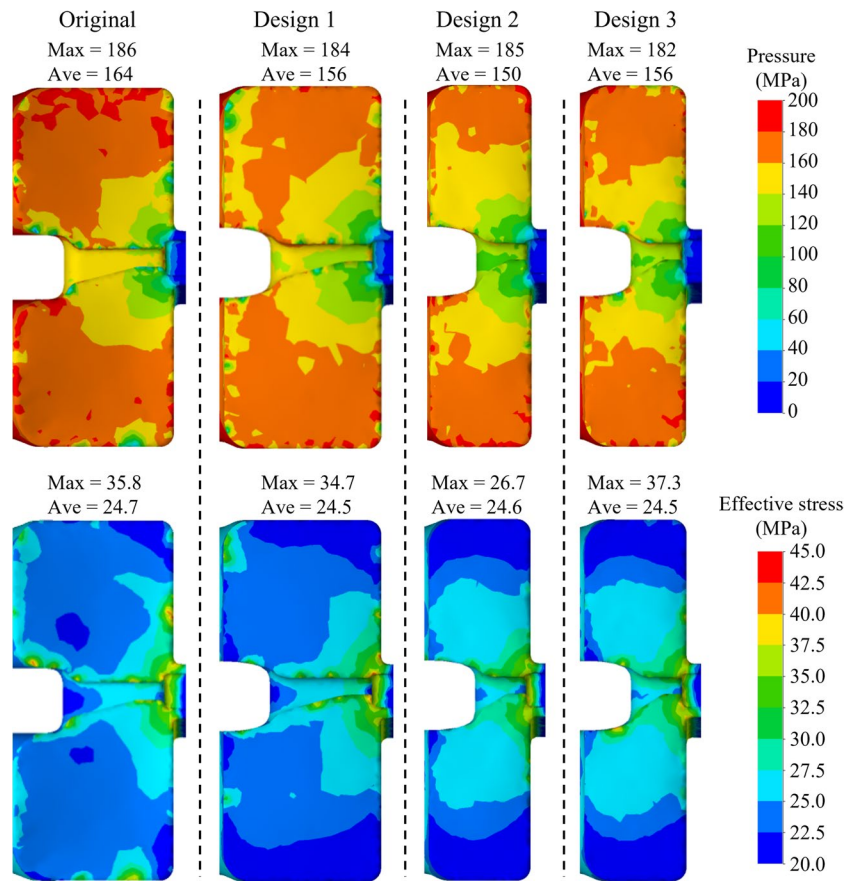


Table 7 Welding related variables for different extrusion designs

	Original design	Design 1	Design 2	Design 3
\bar{p}_{ave}	6.64	6.37	6.10	6.37
σ_{ave}	6.75	6.52	6.30	6.56

Table 8 Performances of the original design and improved Designs 1–3

	Original	Design 1	Design 2	Design 3
Unevenness of the front shape, l	1	0.27	0.47	0.25
Peak stress on extrusion dies	1	0.99	0.97	0.98
Extrusion force	1	0.98	0.96	0.97
Material yield	1	1.90	2.06	2.06
Welding quality, Q	1	0.97	0.93	0.97

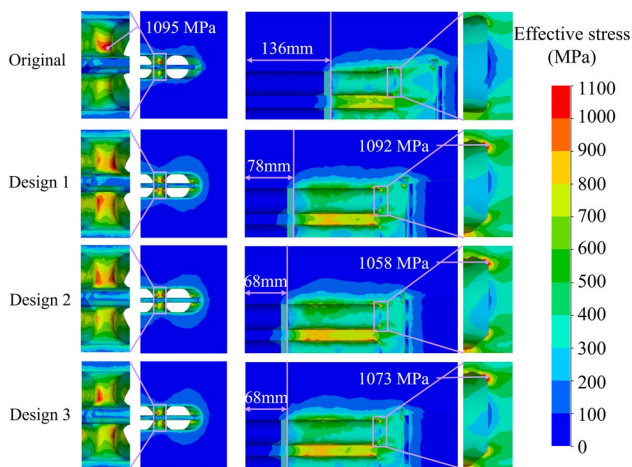


Fig. 15 Effective stress distribution on extrusion dies at the maximum extrusion force for different extrusion designs. The corresponding stem stroke and peak stress of tooling are presented

1 to 0.25 and the material yield is significantly increased from the original 1 to 2.06. Good welding quality can also be obtained in the modified designs. The simulated results demonstrate that the three steps of die design improvements satisfy the optimisation objective, i.e., to enhance the metal flow and material yield within the practical requirements of extrusion force, die lifetime and good welding. It should be noted that in the context of multi-container extrusion method, the area of billet skin per unit volume exceeds that of the porthole extrusion. Thus, the back-end defects in the multi-container extruded profiles could be more significant and further experiments and simulations are required to address this in future research.

Conclusions

In this work, the original three-container extrusion model and six modified models were established for manufacturing thin-walled wide AA6063 hollow profiles. Numerical simulations were conducted to investigate the effects of tooling designs including container diameter, upper die height and welding chamber height on metal flow, extrusion force requirement, welding quality, die safety and material yield. The drawbacks of the original extrusion design were then revealed and a three-step die design optimisation was conducted. Although the final optimised design may be further refined, its improvement is significant especially on the metal flow and material yield, and the improvement process provides effective guidance for the tooling design of multi-container extrusion. The following conclusions are drawn:

- (1) The effect of geometrical variables on metal flow was revealed. After filling the die cavity, the extrusion process includes the breakthrough stage where material starts to exit, the unsteady stage where a whole cross-section of profile can be extruded unevenly and the steady stage where material is extruded with uniform velocity distribution. The inconsistent volume distribution of port-holes in the upper die causes the non-uniform metal flow, especially during breakthrough and unsteady extrusion stages. This unbalanced metal flow results in a 12.4 mm unevenness of the extrudate front shape for the original design and a bigger container diameter or lower welding chamber height can aggravate this inconsistency.
- (2) The geometrical change of the die structure can influence the extrusion force requirement. The most sensitive factor is the container diameter, by increasing which from 34 to 44 mm the deformation-induced force can be significantly raised from 2054 to 2864 kN due to increased extrusion ratio. The dimensions of the upper die and welding chamber have limited influence since they only affect friction.
- (3) Increasing the container diameter and decreasing the upper die and welding chamber height are effective ways to enhance the material yield. Increasing the container diameter from the original 39 mm to 44 mm can increase the material yield by 27%; decreasing the upper die height from the original 90 mm to 65 mm can enhance the material yield by 47%; decreasing the welding chamber height from the original 12 mm to 6 mm can increase the material yield by 14%. However, a bigger container diameter causes higher stress in the areas between containers, and a lower upper die height increases the strength risk of the horizontal bridge.
- (4) Three-step die optimisation was conducted, i.e. the modification of container diameter and upper die in

Design 1, the reduction of welding chamber height in Design 2 and the adjustment of bearing lengths in Design 3. The final improved design (Design 3) is able to decrease the unevenness of the front shape by 75% and double the material yield.

Acknowledgements The authors would like to thank the funding support from UK Engineering and Physical Sciences Research Council (EPSRC) under the Grant Agreement EP/R001715/1 on “LightForm: Embedding Materials Engineering in Manufacturing with Light Alloys” and under EP/X52556X/1 for UKRI Impact Acceleration Funding on Multi-Cylinder Extrusion Technology. J. Lv also greatly appreciates the financial support from the President's PhD Scholarship of Imperial College London.

Author contributions Jiaxin Lv: Methodology, Investigation, Visualization, Data curation, Writing—Original draft preparation. Zhusheng Shi: Conceptualization, Project administration, Supervision, Writing—Reviewing and Editing. Junquan Yu: Methodology, Investigation, Validation, Supervision, Writing—Reviewing and Editing. Weishu Li: Methodology, Investigation. Jianguo Lin: Conceptualization, Funding acquisition, Supervision, Writing—Reviewing and Editing.

Declarations

Competing interests The authors declare that they have no known conflict of interest.

Open Access This article is licensed under a Creative Commons Attribution 4.0 International License, which permits use, sharing, adaptation, distribution and reproduction in any medium or format, as long as you give appropriate credit to the original author(s) and the source, provide a link to the Creative Commons licence, and indicate if changes were made. The images or other third party material in this article are included in the article's Creative Commons licence, unless indicated otherwise in a credit line to the material. If material is not included in the article's Creative Commons licence and your intended use is not permitted by statutory regulation or exceeds the permitted use, you will need to obtain permission directly from the copyright holder. To view a copy of this licence, visit <http://creativecommons.org/licenses/by/4.0/>.

References

1. Wanhill RJH (2014) Chapter 15 - Aerospace Applications of Aluminum-Lithium Alloys. In: Eswara Prasad N, Gokhale AA, Wanhill RJH (eds) Aluminum-lithium Alloys. Butterworth-Heinemann, Boston, pp 503–535
2. Hashimoto N (2017) Application of aluminum extrusions to automotive parts. *Kobelco Technol Rev* 35:69–75
3. Wahid MA, Siddiquee AN, Khan ZA (2020) Aluminum alloys in marine construction: characteristics, application, and problems from a fabrication viewpoint. *Marine Syst Ocean Technol* 15:70–80. <https://doi.org/10.1007/s40868-019-00069-w>
4. Zhao G, Chen H, Zhang C, Guan Y, Anjiang G, Peng L (2014) Die optimization design and experimental study of a large wallboard aluminum alloy profile used for high-speed train. *Int J Adv Manuf Technol* 74:539–549. <https://doi.org/10.1007/s00170-014-5903-7>

5. Barbara R, Lorenzo D, Luca T (2017) Multi-goal optimization of industrial extrusion dies by means of meta-models. *Int J Adv Manuf Technol* 88:3281–3293. <https://doi.org/10.1007/s00170-016-9009-2>
6. Lee DH, Kim YJ, Kim S-H, Moon BG, Park SH (2021) Extrusion limit diagram of AZ91–0.9Ca–0.6Y–0.5MM alloy and effects of extrusion parameters on its microstructure and mechanical properties. *J Magnes Alloys*. <https://doi.org/10.1016/j.jma.2021.06.002>
7. Zhang C, Zhao G, Guan Y, Gao A, Wang L, Li P (2015) Virtual tryout and optimization of the extrusion die for an aluminum profile with complex cross-sections. *Int J Adv Manuf Technol* 78:927–937. <https://doi.org/10.1007/s00170-014-6691-9>
8. Giarmas E, Tzetzis D (2022) Optimization of die design for extrusion of 6xxx series aluminum alloys through finite element analysis: a critical review. *Int J Adv Manuf Technol* 119:5529–5551. <https://doi.org/10.1007/s00170-022-08694-3>
9. Donati L, Tomesani L (2008) Seam welds modeling and mechanical properties prediction in the extrusion of AA6082 alloy. *Key Engineering Materials Trans Tech Publ*, pp 125–136. <https://doi.org/10.4028/www.scientific.net/KEM.367.125>
10. Truong T-T, Hsu Q-C, Tong V-C (2020) Effects of solid die types in complex and large-scale aluminum profile extrusion. *Appl Sci* 10:263. <https://doi.org/10.3390/app10010263>
11. Liu J (1999) Aluminum extrusion die design, manufacture, use and maintenance. Metallurgical Industry Press of China, Beijing, China
12. Chen H, Zhao G, Zhang C, Guan Y, Liu H, Kou F (2011) Numerical simulation of extrusion process and die structure optimization for a complex aluminum multicavity wallboard of high-speed train. *Mater Manuf Process* 26:1530–1538. <https://doi.org/10.1080/10426914.2011.551950>
13. Donati L, Tomesani L (2004) The prediction of seam welds quality in aluminum extrusion. *J Mater Process Technol* 153–154:366–373. <https://doi.org/10.1016/j.jmatprotec.2004.04.215>
14. Liu J, Lin G-y, Feng D, Zou Y-m, Sun L-p (2010) Effects of process parameters and die geometry on longitudinal welds quality in aluminum porthole die extrusion process. *J Cent South Univ Technol* 17:688–696. <https://doi.org/10.1007/s11771-010-0541-1>
15. Khan YA, Valberg HS, Jacobsen BOT (2010) Deformation conditions in the extrusion weld zone when using pointed and square ended bridge. *Int J Mater Form* 3:379–382. <https://doi.org/10.1007/s12289-010-0786-0>
16. Wang Y, Zang A, Mahmoodkhani Y, Wells M, Poole W, Parson N (2021) The effect of bridge geometry on microstructure and texture evolution during porthole die extrusion of an Al–Mg–Si–Mn–Cr alloy. *Metall Mater Trans A* 52:3503–3516. <https://doi.org/10.1007/s11661-021-06322-5>
17. Yi J, Wang Z-h, Liu Z-w, Zhang J-m, He X (2018) FE analysis of extrusion defect and optimization of metal flow in porthole die for complex hollow aluminium profile. *T Nonferr Metal Soc* 28:2094–2101. [https://doi.org/10.1016/S1003-6326\(18\)64853-8](https://doi.org/10.1016/S1003-6326(18)64853-8)
18. Lu X, Zhang C, Zhao G, Guan Y, Chen L, Gao A (2016) State-of-the-art of extrusion welding and proposal of a method to evaluate quantitatively welding quality during three-dimensional extrusion process. *Mater Des* 89:737–748. <https://doi.org/10.1016/j.matdes.2015.10.033>
19. Sun X, Zhao G, Zhang C, Guan Y, Gao A (2013) Optimal design of second-step welding chamber for a condenser tube extrusion die based on the response surface method and the genetic algorithm. *Mater Manuf Process* 28:823–834. <https://doi.org/10.1080/10426914.2012.736657>
20. Wu X, Zhao G, Luan Y, Ma X (2006) Numerical simulation and die structure optimization of an aluminum rectangular hollow pipe extrusion process. *Mater Sci Eng A* 435–436:266–274. <https://doi.org/10.1016/j.msea.2006.06.114>
21. Zhang C, Zhao G, Chen Z, Chen H, Kou F (2012) Effect of extrusion stem speed on extrusion process for a hollow aluminum profile. *Mater Sci Eng, B* 177:1691–1697. <https://doi.org/10.1016/j.mseb.2011.09.041>
22. Jo HH, Jeong CS, Lee SK, Kim BM (2003) Determination of welding pressure in the non-steady-state porthole die extrusion of improved Al7003 hollow section tubes. *J Mater Process Technol* 139:428–433. [https://doi.org/10.1016/S0924-0136\(03\)00518-1](https://doi.org/10.1016/S0924-0136(03)00518-1)
23. Gagliardi F, Schwane M, Citrea T, Haase M, Khalifa NB, Tekkaya AE (2014) Bridge design influences on the pressure conditions in the welding chamber for porthole die extrusion. *Key Eng Mater* 622:87–94. <https://doi.org/10.4028/www.scientific.net/KEM.622-623.87>
24. Lv J, Yu J, Shi Z, Li W, Lin J (2023) Feasibility study of a novel multi-container extrusion method for manufacturing wide aluminium profiles with low force. *J Manuf Process* 85:584–593. <https://doi.org/10.1016/j.jmapro.2022.11.055>
25. Lv J, Shi Z, Yu J, Li W, Lin J (2023) Analysis of solid-state welding in extruding wide aluminium hollow profiles using a new three-container extrusion system. *J Mater Process Technol* 94:146–158. <https://doi.org/10.1016/j.jmapro.2023.03.048>
26. QForm metal forming simulation software. Micas Simulations Limited. <https://www.qform3d.com/>. Accessed 3 Jul 2023
27. Wang Y, Zhao G, Sun L, Wang X, Lv Z, Sun Y (2023) Effects of billet heating temperature and extrusion speed on the microstructures and mechanical properties of the longitudinal welds in aluminum alloy profiles with complex cross-section. *Vacuum* 207:111578. <https://doi.org/10.1016/j.vacuum.2022.111578>
28. Donati L, Tomesani L, Minak G (2007) Characterization of seam weld quality in AA6082 extruded profiles. *J Mater Process Technol* 191:127–131. <https://doi.org/10.1016/j.jmatprotec.2007.03.073>
29. Gagliardi F, Ciancio C, Ambrogio G (2018) Optimization of porthole die extrusion by Grey-Taguchi relational analysis. *Int J Adv Manuf Technol* 94(1):719–728. <https://doi.org/10.1007/s00170-017-0917-6>
30. Xue X, Vincze G, Pereira AB, Pan J, Liao J (2018) Assessment of metal flow balance in multi-output porthole hot extrusion of AA6060 thin-walled profile. *Metals* 8. <https://doi.org/10.3390/met8060462>
31. Zhao Y, Pei J-y, Guo L-l, Yun X-b, Ma H-c (2021) Effects of extrusion speed of continuous extrusion with double billets on welding performance of 6063 Al alloy. *T Nonferr Metal Soc* 31:1561–1571. [https://doi.org/10.1016/S1003-6326\(21\)65598-X](https://doi.org/10.1016/S1003-6326(21)65598-X)

Publisher's Note Springer Nature remains neutral with regard to jurisdictional claims in published maps and institutional affiliations.